Uniformity and asymmetry of rapid curved-line detection explained by parallel categorical coding of contour curvature

David H. Foster *, C. Julie Savage

Visual and Computational Neuroscience Group, Department of Optometry and Neuroscience, University of Manchester Institute of Science and Technology, Manchester M60 1QD, UK

Received 1 November 2001; received in revised form 17 May 2002

Abstract

The aim of this work was to elucidate several characteristic phenomena associated with rapid curved-line detection in multi-element arrays and to provide a unified account of the underlying curvature-sensitive mechanisms. To this end, a parametric experiment was performed in which the detectability of a curved-line target in a briefly presented planar array of curved-line distractors was measured for a range of target and distractor curvatures and distractor numbers. For both vertically oriented and randomly oriented curved lines, it was found that (1) the dependence of target detectability on target curvature was independent of distractor number for small distractor curvatures but not for medium-to-large distractor curvatures; (2) an asymmetry in target detectability with respect to interchange of target and distractor curvatures occurred only with large distractor numbers; and (3) with small distractor numbers, target detectability depended only on the difference between target and distractor curvatures. These properties of spatial parallelism, asymmetry, and uniformity were explained quantitatively by a minimal model of rapid curved-line detection in which contour curvature was coded in terms of just two or three curvature categories, depending on curved-line orientation.

© 2002 Elsevier Science Ltd. All rights reserved.

Keywords: Parallel processing; Categorical coding; Search; Pop-out; Asymmetry

1. Introduction

Along with differences in line orientation, differences in line curvature are highly salient in visual scene analysis (Attneave, 1954). A curved-line "target" can be readily detected within a planar array of straight-line distractors, even when the display lasts a tenth of a second and is followed by a masking field (Foster, 1983); phenomenologically, a curved-line target produces visual "pop-out" (Li, 1999; Treisman, 1985). Moreover, when display duration is unlimited, the time taken to search for a curved-line target is little affected by the number of straight-line distractors (Treisman & Gormican, 1988), suggesting that processing is mediated by mechanisms acting spatially in parallel over the visual field (Bergen & Julesz, 1983; Treisman, Sykes, & Gelade, 1977). Although oriented-line-target detection shows similar properties, the mechanisms underlying curved-line-target detection may have a specific sensitivity to contour curvature (Treisman & Gormican, 1988; Wolfe, Friedman-Hill, Stewart, & O'Connell, 1992a), rather than representing a generalized response to elementary orientation cues (Blakemore & Over, 1974).

Yet relatively little is known about the spatial characteristics of rapid curved-line detection, despite a long history of research into curved-line discrimination with sparse, long-duration stimuli (e.g. Andrews, Butcher, & Buckley, 1973; Bühler, 1913; Della Valle, Andrews, & Ross, 1956; Foster, Simmons, & Cook, 1993; Kramer & Fahle, 1996, 1998; Ogilvie & Daicar, 1967; Watt, 1984; Watt & Andrews, 1982; Watt, Ward, & Casco, 1987; Whitaker, Latham, Makela, & Rovamo, 1993; Whitaker & McGraw, 1998; Wilson, 1985; Wilson & Richards, 1989; Zanker & Quenzer, 1999). There is some evidence from previous studies of rapid curved-line detection that the underlying mechanisms may code contour curvature discretely, yielding just a few probabilistically generated perceptual categories (e.g. Ferraro & Foster, 1986; Foster, 1983). There is also some evidence of categorical coding of contour curvature in

---

* Corresponding author. Tel.: +44-161-200-3888; fax: +44-161-200-3887.

E-mail address: d.h.foster@umist.ac.uk (D.H. Foster).

texture segmentation (Simmons & Foster, 1992; although see Beck, 1973). As with oriented-line-target detection (e.g. Carrasco, Mclean, Katz, & Frieder, 1998; Doherty & Foster, 2001; Foster & Ward, 1991; Foster, Savage, Mannan, & Ruddock, 2000; Treisman & Gormican, 1988; Wolfe et al., 1992a), there is a striking asymmetry with respect to interchanging target and distractor identities: a curved-line target is easier to detect in a background of straight-line distractors than vice-versa (Gurnsey, Humphrey, & Kapitan, 1992; Treisman & Gormican, 1988).

The aim of the present work, therefore, was to place these phenomena associated with rapid curved-line detection—pop-out, parallel search, perceptual categorization, and target–distractor asymmetry—within a common explanatory framework, and to provide a unified account of the underlying mechanisms, in particular, what form their curvature-tuning functions take and how such mechanisms might operate in concert to produce a rapid response independent of distractor number.

The experimental approach was parametric. A high-resolution graphics display system was used to determine the visual detectability of a curved-line target as a function both of its curvature and of the curvature of curved-line distractors in brief stimulus arrays, as illustrated in Fig. 1. Curved lines were oriented either vertically, as in Fig. 1A, or randomly, as in Fig. 1B. These two orientation configurations were used to test whether target-detection performance was confounded by curved-line orientation (Simmons & Foster, 1992). The number of curved lines in each array varied from 2 to 20. Performance was quantified in terms of the bias-free measure d' from signal-detection theory rather than in terms of response time, thus emphasizing encoding-level processes rather than decision-level processes (Rouder, 2000). From these data, a minimal computational model of detection performance was constructed, from which the characteristics of the underlying curvature-sensitive mechanisms could be inferred.

2. Experimental methods

2.1. Stimuli

Each stimulus display consisted of 2, 3, 5, 10, or 20 curved lines, with chord lengths 1° visual angle, distributed randomly within a circular field of diameter 20° in the frontoparallel plane. The thickness of each curved line was 3–4 arcmin. All of the curved lines in the display had the same curvature, except for the target, which was present in 50% of trials. When the target was absent, it was replaced by a distractor so that target and non-target displays had the same number of curved lines. The centre-to-centre spacing between any pair of curved

lines was at least 2°, so that there was at least 1° between their closest points. The position of the target was limited to an annular field, centred on the fixation point, with inner and outer diameter 6° and 16° (Sagi & Julesz, 1987); observers were not informed of this constraint.

Each curved line was generated by affinely interpolating between a fixed straight line of length 1° and a fixed circular arc of chord length 1° and turning angle 120° in the frontoparallel plane (the difference in angle between the tangents at the two ends). This method of curved-line generation, which produces elliptical approximations to true circular arcs, has the theoretical advantage of defining a transformationally uniform stimulus continuum, [1] although over the range of stimuli used here, the maximum departure from circularity was less than 3%. Curvature was quantified in terms of the parameter sag, which measures the maximum deviation from linearity of the curve, here the distance c in visual angle between the midpoint of the curve and the midpoint of its chord, as shown in Fig. 2. As Andrews et al. (1973) noted, however, this need not suggest that all deviations from linearity are coded in the same way by the visual system: once a difference in deviation has been detected, the variety may be identified by other mechanisms. With the stimulus continuum just defined, it has been shown (Foster et al., 1993) that sag provides the best cue in accounting for the discriminability of pairs of long-duration, curved-line stimuli, over a range of one- and two-dimensional transformations. The "best" cue was interpreted in the sense of statistical estimation theory, that is, associated with the least variance in the data. In this respect, sag is better than some of its covariates, including Euclidean curvature (the reciprocal of the radius of curvature of the curved line), turning angle, arc-length, and several others, which provide poor predictors of discrimination performance. These covariates were therefore ignored in the present experiment (cf. Treisman & Gormican, 1988).

In each trial, the sag values of the distractors were drawn randomly from the range 0, 2.5, 5.0, 7.5, 10.0, 12.5, 15.0 arcmin and the sag values of the targets randomly from the range 0, ±5.0, ±10.0, ±15.0, ±20.0 arcmin (negative values, signifying curvature in the opposite direction, were defined only when all the curved lines were oriented vertically). When all the curved lines were oriented vertically, the common direction of

---

[1] A transformationally uniform scale is a sensible prerequisite for demonstrating categorical behaviour (Foster, 1980; Foster, 1983; Shepard & Cermak, 1973). On such a scale, the same spatial transformation relates any pair of curved-line elements separated by the same distance along the scale, independent of where they are located on the scale. Thus, if c_s and $c_{s+\Delta s}$ are curves with scale parameter values s and $s + \Delta s$, respectively, related by a transformation T, that is, $c_{s+\Delta s} = Tc_s$, then, for any other scale parameter value s' for which the curves $c_{s'}$ and $c_{s'+\Delta s}$ are defined, it follows that $c_{s'+\Delta s} = Tc_{s'}$.
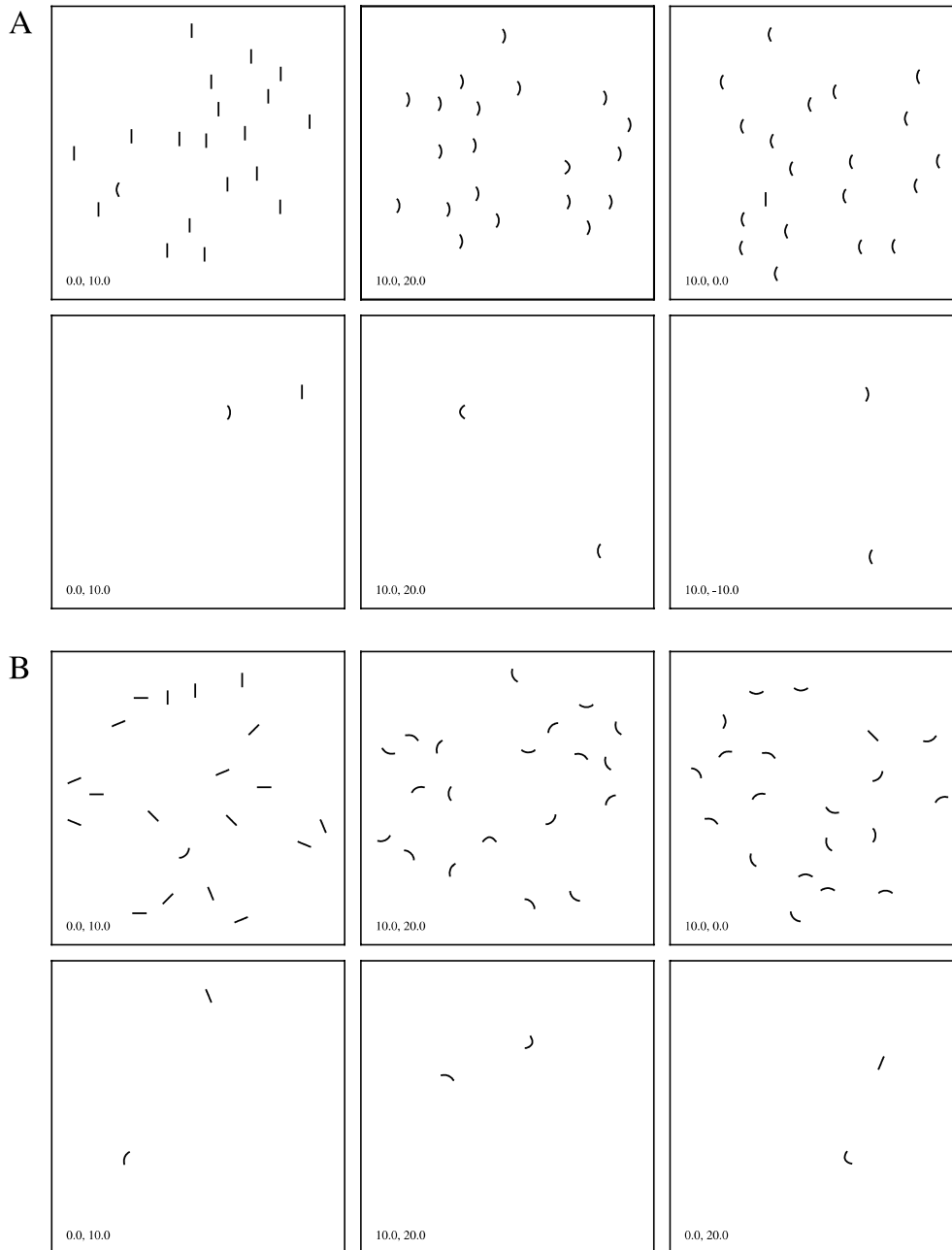
Fig. 1. Examples of target arrays of curved lines, oriented either A vertically or B randomly. In the experiment, the number of curved lines in each array varied from 2 to 20. The examples in both A and B are for target and distractor sag values of 0, 10, and 20 arcmin (the numbers on the lower left of each panel show the actual combinations of distractor and target values in arcmin, not shown in the experiment). The plots are to scale and contrast-reversed.

curvature of the distractors and the direction of the target with respect to the distractors were chosen randomly in each trial. When the curved lines were randomly oriented, their individual orientations were chosen randomly from the range $0°, 22.5°, \ldots, 337.5°$ in the frontoparallel plane.

The examples in Fig. 1 are for target and distractor sag values of 0, 10, and 20 arcmin (the numbers on the lower left of each panel indicate the actual combinations of distractor and target values in arcmin, not shown of

course in the experiment). The plots are contrast-reversed.

Stimuli were white and appeared superimposed on a uniform grey $30° \times 35°$ background field with luminance about 40 cd m^{-2}. The duration of the stimulus display was 100 ms, and it was followed by a blank field lasting 100 ms, and then by a masking field lasting 500 ms. The purpose of the mask was to limit the effective display duration (i.e. the time available for inspection of the fading after-image of the curved lines). The mask
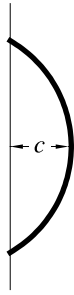
Fig. 2. Parameterization of curvature. Curvature was quantified in terms of sag c ("sagitta", Della Valle et al., 1956), which measures the maximum deviation from linearity of a curve, here the distance in visual angle between the midpoint of the curve and the midpoint of its chord.

consisted of patches of oriented lines, with the arrangement of the lines differing from patch to patch and each patch covering one of the previously displayed curved lines. The stimulus time course was chosen on the basis of previous experiments (e.g. Foster, 1983).

2.2. Apparatus

Stimuli were generated on the screen of a 21-in cathode-ray tube (CRT) (Hewlett-Packard, USA; Type 1321A, white P4 sulfide phosphor, measured 90%–10% decay time less than 100 μs, rise time less than decay time) controlled by a 10-bit vector-graphics generator (Sigma Electronic Systems, UK; QVEC 2150) and additional 12-bit digital-to-analogue converters, in turn controlled by a laboratory computer. Each curved line consisted of a sequence of 23–30 points (depending on arc length) plotted on the screen within an invisible square patch of side 12.5 mm with a local linear precision of 1 part in 1024 horizontally and vertically. The intensity per unit length of the curved lines was independent of the curvature of the line and of its orientation. Despite their punctate structure, the curved lines appeared smooth to the eye. [2]

Each patch containing each curved-line was positioned on the screen with a global linear precision of 1 part in 4096 horizontally and vertically. The maximum number of curved lines used in the experiment could all be plotted on the screen within one 20 ms refresh interval. The nominal 100 ms presentation time thus comprised 5 refresh cycles. This fine temporal structure was not apparent to the observer.

The CRT screen was viewed binocularly at a distance of 0.5 m through a view-tunnel and optical system that produced the uniformly illuminated background upon which the stimuli appeared superimposed. The observer's head was steadied with a chinrest and head-

rest. Before each experimental session, the CRT was allowed to warm-up for 30 min and its spatial calibration was then adjusted by aligning a test image against fiducial marks on a transparent template attached temporarily to the screen.

2.3. Procedure

The task of the observer was to report whether any one of the curved lines in the stimulus display differed from the others in being more or less curved or, when all the curved lines were oriented vertically, in pointing in the opposite direction. The order of operations in each trial was as follows. The observer fixated a fixation cross on the CRT screen, and, when ready, initiated a trial by pressing a switch on a push-button box connected to the computer. The fixation cross disappeared, and, after a 40 ms delay, the curved-line stimulus appeared, followed by the blank field, and then the masking field. When the observer had responded using the push-button box, the fixation target reappeared after about a 2 s delay, indicating that the next trial could be initiated. Central fixation was maintained during the presentation period. Observers were encouraged to respond as quickly as was consistent with accuracy.

Fresh randomly selected stimulus displays (and masks) were generated in every trial. Trials were organised into subblocks each comprising 7 practice trials (the results of which were discarded) and 70 recorded trials, in which the number of curved lines in each display was constant. Each block of trials consisted of 5 such subblocks, each with a different number of curved lines (2, 3, 5, 10, or 20), in random order. Three blocks of trials were normally performed in a single 1 h experimental session. For each observer, each combination of target and distractor curvature appeared 15 times in target displays and each distractor curvature appeared in the same number of non-target displays. The total number of trials performed by each observer was therefore $15 \times 2 \times 5 \times 7 \times 9 = 9540$ (5 numbers of curved lines, 7 distractor curvatures, 9 target curvatures) for vertically oriented curved lines and $15 \times 2 \times 5 \times 7 \times 5 = 5250$ (5 numbers of curved lines, 7 distractor curvatures, 5 target curvatures) for randomly oriented curved lines.

At the beginning of each experimental session, the intensity of the stimuli was adjusted to be 10 times luminance increment threshold, so that the stimuli were adequately suprathreshold, but not so bright as to produce noticeable after-images. [3]

---

[2] As a control on the fidelity of the stimuli, they were photographed at their display durations and the photographic images measured and compared with their specifications.

[3] In this adjustment, a 1-log-unit neutral-density filter was placed between the CRT screen and view-tunnel, thereby leaving the background unattenuated; the luminance of the attenuated stimuli was set to the observer's threshold on that background; and the neutral-density filter was then removed.

2.4. Subjects

There were 6 observers, three male and three female. Each had normal or corrected-to-normal vision (Snellen acuity $\geqslant 6/6$ and optometrically verified astigmatism $\leqslant 0.25$ DC). They were aged 19–29 yr, and, except for one (coauthor CJS), they were unaware of the purpose of the experiment and were paid for their participation.

2.5. Data analysis

As indicated earlier, target detectability at each combination of distractor and target curvature was summarized by the discrimination index d' (Green & Swets, 1966). In brief, if HR is the detection hit rate, FAR the false-alarm rate, and z is the inverse of the cumulative unit normal distribution, then $d' = z(\text{HR}) - z(\text{FAR})$. In this way, d' linearizes and combines re-sponses to target and non-target displays. If certain conditions on the underlying psychophysical mecha-nisms are satisfied, then d' provides a measure that is independent of observer bias (Green & Swets, 1966). Values of d' were averaged over observers, and each mean was therefore based on $6 \times 30 = 180$ trials in all. When the curved lines were all vertical, results for di-stractors with the same magnitude but different direction of curvature were pooled, retaining information about the relative direction of target curvature.

3. Curved-line detection performance

3.1. Vertically oriented curved lines

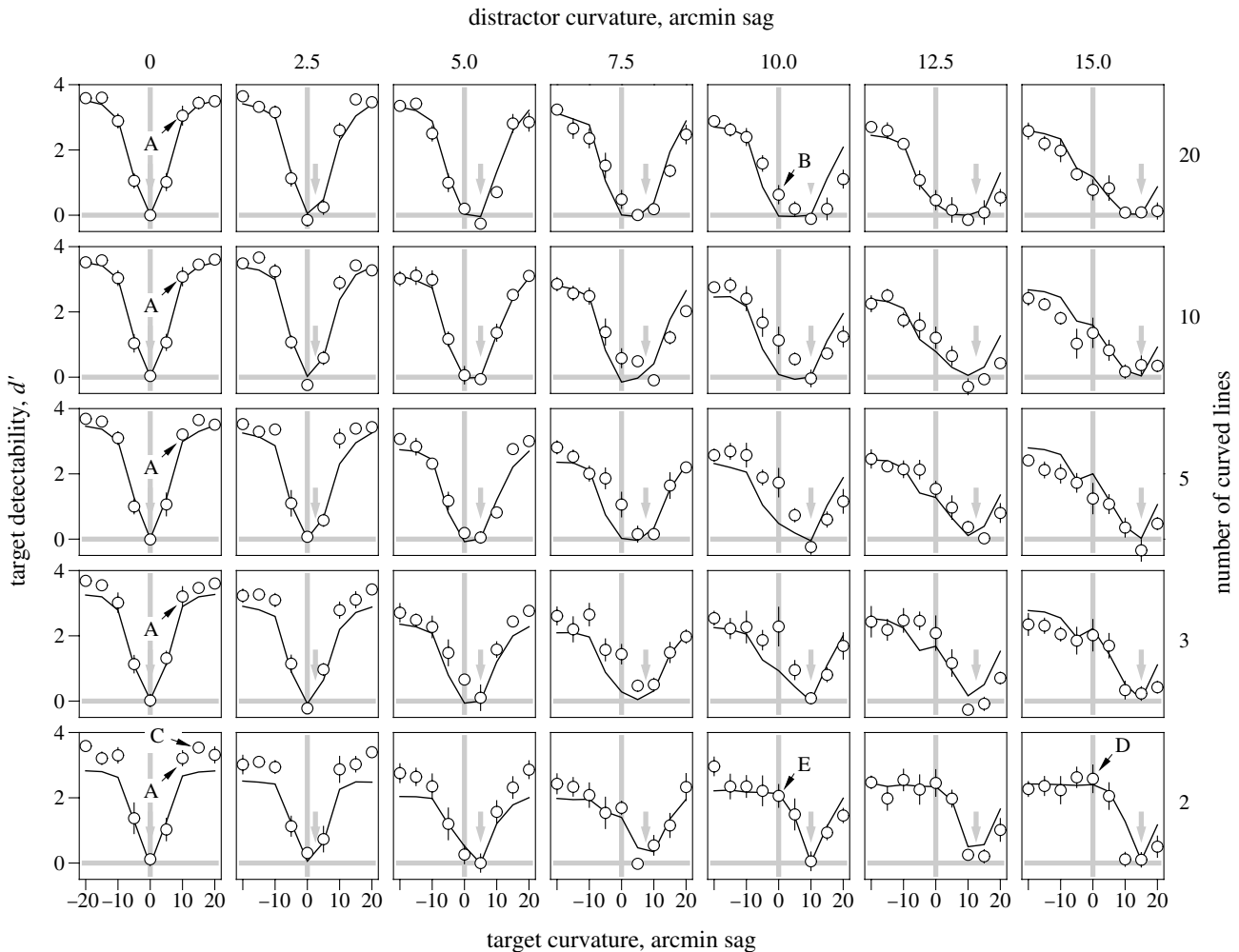Fig. 3 shows mean target detectability (open circles) as a function of target curvature for vertically oriented

Fig. 3. Target detectability as a function of target curvature for vertically oriented curved lines. In each panel, the symbols show values of d' averaged over six observers, with the vertical bars where sufficiently large representing ±1 SEM. The columns of panels correspond to different distractor curvatures (indicated by the grey vertical arrows in the panels), and the rows of panels to different numbers of curved lines in the stimulus array (indicated by the column of numbers on the right of the figure). The continuous lines were derived from a categorical model of curved-line detection. The points indicated by letters are discussed in the text.

curved lines. Each panel represents a target-detection function for a different experimental condition: the columns of panels correspond to different distractor curvatures (indicated by the grey vertical arrows in the panels) and the rows of panels to different numbers of curved lines. The continuous lines in the panels are from a model of curved-line detection described later. In all conditions, discrimination index d' increased monotonically with increasing difference between target and distractor curvatures.

To aid interpretation, consider the following specific instances of performance. First, the points labelled A in the leftmost column illustrate spatially parallel detection: the value of the discrimination index d' is almost exactly constant as the number of curved lines increases from 2 at the bottom to 20 at the top (the gradient of the linear trend is less than -0.01). Second, the points labelled A and B in the top row illustrate target–distractor asymmetry: A is for a target with a curvature of 10 arcmin and distractors with a curvature of 0 arcmin ($d' = 3.05$); and B is for a target with a curvature of 0

arcmin and distractors with a curvature of 10 arcmin ($d' = 0.63$).

The complete target-detection functions in each panel generalize these specific instances. Thus, for distractor curvatures at or close to zero (the two leftmost columns), the target-detection function is almost independent of the number of distractors. This uniformity in performance is shown more clearly by a calculation of residuals. At each target and distractor curvature, let $\overline{d'}$ be the value of d' averaged over distractor number. Fig. 4 shows the residuals d'–$\overline{d'}$ as a function of target curvature. They are largely constant and equal to zero over distractor number at distractor curvatures of 0–2.5 arcmin, but reveal systematic variation at distractor curvatures of about 5.0–7.5 arcmin, which increases at still larger distractor curvatures.

That vertically oriented curved-line targets in vertically oriented straight- or almost-straight-line distractors are processed in parallel was not unexpected (Treisman & Gormican, 1988; Wolfe, Yee, & Friedman-Hill, 1992b). By virtue of the uniformity at small dis-
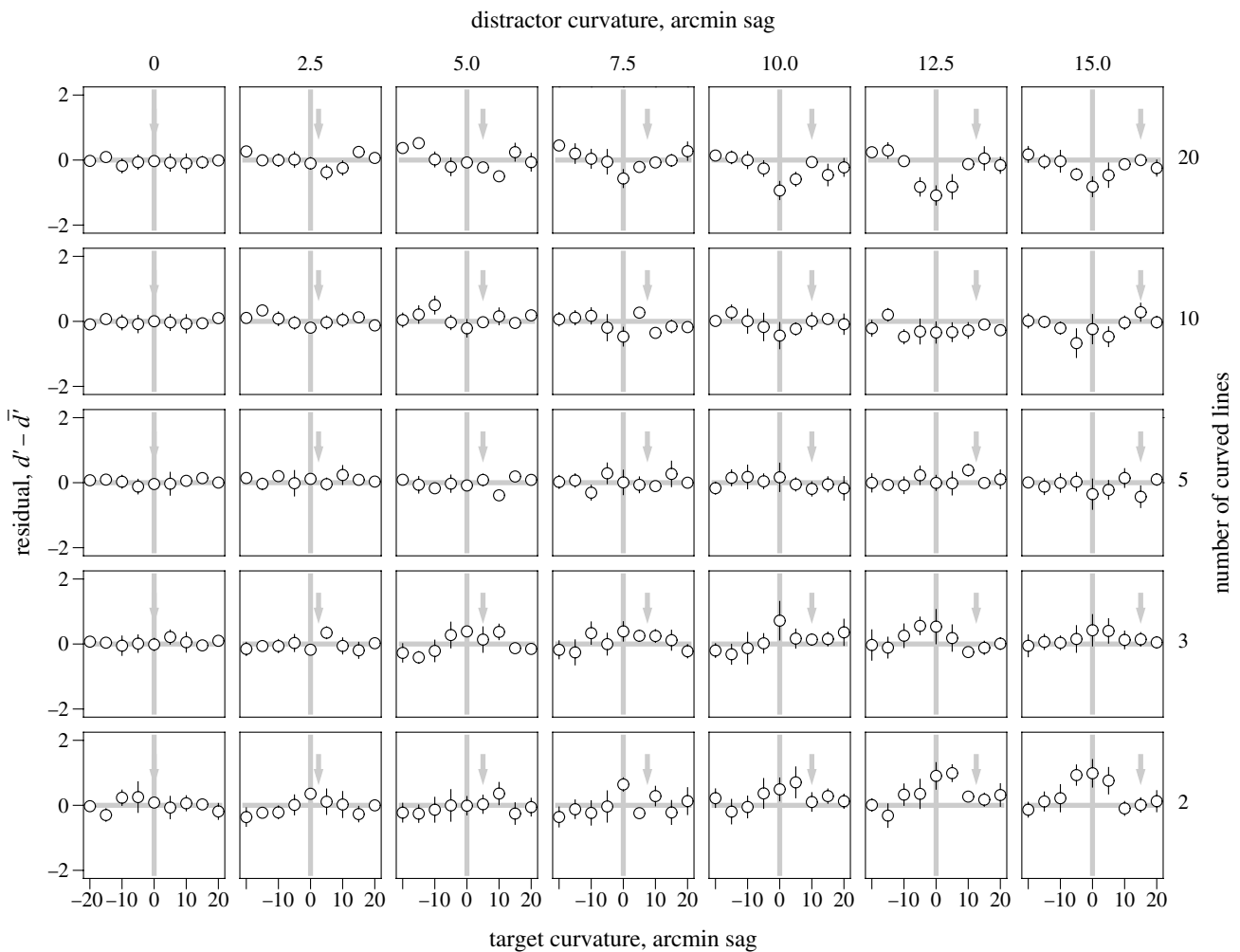

Fig. 4. Uniformity of target-detection functions for vertically oriented curved lines. Residuals $d' - \overline{d'}$ from Fig. 3 are plotted as a function of target curvature, where each $\overline{d'}$ is the average of d' over distractor number. Other details as for Fig. 3.
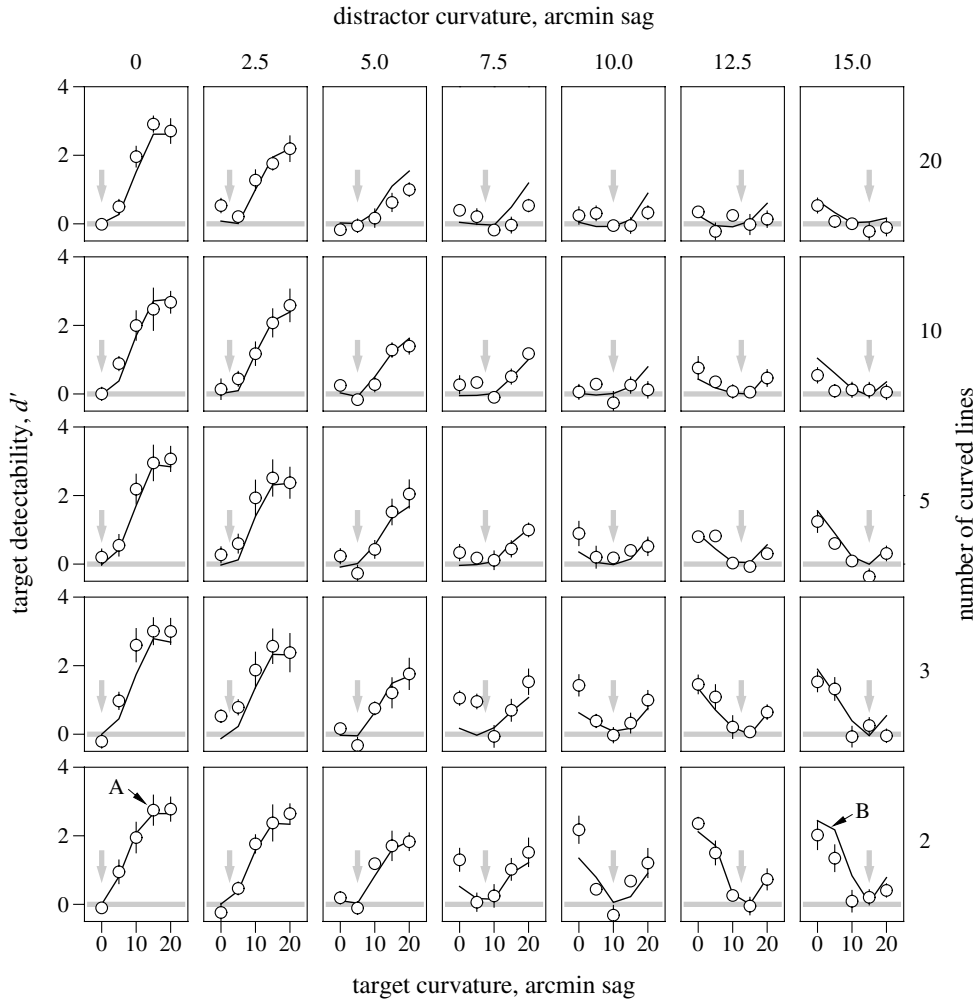
Fig. 5. Target detectability as a function of target curvature for randomly oriented curved lines. Only positive values of target curvature are plotted, as the direction of target curvature with respect to distractor curvature was not constant. Other details as for Fig. 3.

tractor curvatures of the target-detection function, the values of which range over d' values of about 1.0 to 3.5, such processing seems not to depend on the task difficulty as reflected in level of performance (see e.g. Foster & Simmons, 1994), although it was not tested here for d' values closer to 0. In contrast, for distractor curvatures at or close to the maximum (the two rightmost columns in Figs. 3 and 4), the target-detection function does depend on the number of distractors, most obviously at target curvatures close to 0 arcmin. This shift from parallel to non-parallel processing with distractor curvature, along with other qualitative features of the data, is analysed in more detail in Section 3.3 and subsequently.

3.2. Randomly oriented curved lines

Fig. 5 shows mean target detectability as a function of target curvature for randomly oriented curved lines. Only positive values of target curvature are plot-

ted, as the direction of target curvature with respect to the distractor curvature was not defined. As in Fig. 3, the columns of panels correspond to different distractor curvatures (indicated by the grey vertical arrows in the panels) and the rows of panels to different numbers of curved lines. The continuous lines in the panels are from a model of curved-line detection described later.

Despite the variation in orientation of the target and distractors, the target-detection functions are similar to the corresponding sections of those for vertically oriented curved lines (Fig. 3), although the slopes of the functions are here less sharp. For distractor curvatures at or close to zero (the two leftmost columns), the target-detection function is almost independent of the number of curved lines as that number varies from 2 to 20. Fig. 6 shows the residuals $d'-\overline{d'}$ as a function of target curvature. As with vertically oriented curved lines, the residuals are largely constant and equal to zero over distractor number at distractor curvatures of 0–2.5
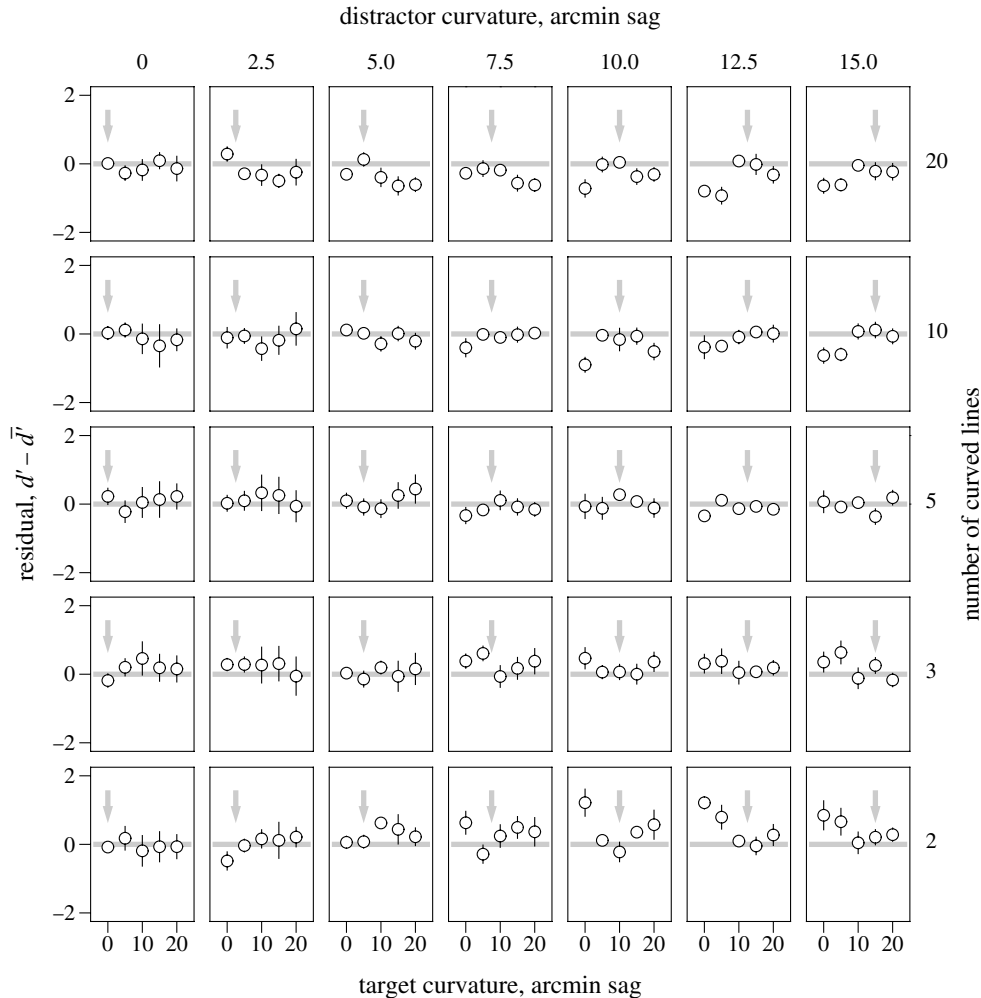
Fig. 6. Uniformity of target-detection functions for randomly oriented curved lines. Residuals $d' - \overline{d'}$ from Fig. 5 are plotted as a function of target curvature, where each $\overline{d'}$ is the average of d' over distractor number. Other details as for Fig. 3.

arcmin, but reveal systematic variation at distractor curvatures of about 5.0–7.5 arcmin, which increases at still larger distractor curvatures.

3.3. Uniformities and asymmetries of target detection

The variations of target detectability with target and distractor curvatures and distractor number shown in Fig. 3 for vertically oriented curved lines and in Fig. 5 for randomly oriented curved lines have certain common features: (1) the approximate uniformity of the dependence of target detectability on target curvature over distractor number at small distractor curvatures (leftmost two columns), but not at medium-to-large distractor curvatures (middle-to-rightmost columns); (2) the asymmetry in target detectability with respect to interchange of target and distractor curvatures for large distractor numbers (top row); and (3) the approximate uniformity of the dependence of target detectability on the difference between target and distractor curvatures

over distractor curvature for small distractor numbers (bottom row). [4]

In addition to the main asymmetry with large distractor numbers, there is a secondary asymmetry with small distractor numbers. For pairs of vertically oriented curved lines (Fig. 3, bottom row), target detectability appears to be higher with target and distractor curvatures of respectively 15 and 0 arcmin (leftmost panel, data point C) than with target and distractor curvatures of respectively 0 and 15 arcmin (rightmost panel, data point D). Yet, experimentally, these target arrays were indistinguishable. The difference can be traced to the FAR computed for the corresponding non-target arrays: it was slightly higher when the distractor curvature was 15 arcmin than when it was 0 arcmin. The

---

[4] Symbolically, if d' is written as a function f of target curvature c_t, distractor curvature c_d, and number of distractors n, that is, $d' = f(c_t, c_d, n)$, then, in the limit, (1)–(3) are equivalent to the following: (1) $f(c_t, 0, n) = f(c_t, 0, 1)$, for all c_t and n; (2) $f(c_t, c_d, 19) \neq f(c_d, c_t, 19)$, for all $c_t \neq c_d$; and (3) $f(c_t, c_d, 1) = f(c_t - c_d, 0, 1)$, for all c_t, c_d.

effect is not due to chance; for it exists with other target–distractor pairs (e.g. data points A and E). It also holds for pairs of randomly oriented curved lines (Fig. 5, bottom row, e.g. data points A and B).

4. Curvature-sensitive mechanisms

Is it possible to represent this pattern of target-detection performance in terms of the activity of a single discrete population of curvature-sensitive mechanisms? The factors to address include (i) the possible receptive-field structures of these mechanisms; (ii) the kinds of curvature-tuning functions relating mechanism activity to stimulus curvature; and (iii) a rule for generating hit and false-alarm responses from activated mechanisms.

4.1. Receptive-field structures

Several types of contour-curvature-sensitive mechanisms have been proposed. In approximate order of selectivity, these include (1) line-sensitive units (Wilson, 1985); (2) end-inhibited line-sensitive units (Dobbins, Zucker, & Cynader, 1987, 1989; Wiesel & Gilbert, 1989); (3) 2×3 matrices of excitatory and inhibitory units (Koenderink & van Doorn, 1987, 1992b), an example of which is illustrated in Fig. 7A; and (4) non-collinear line-
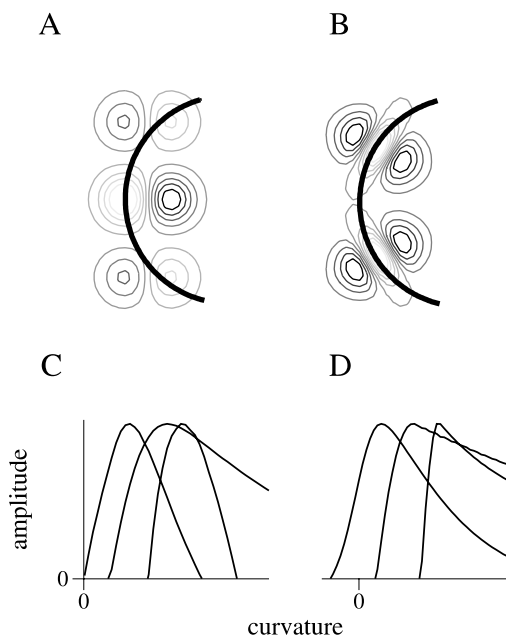
A   B

C   D

Fig. 7. A and B, receptive-field structures of two classes of contour-curvature-sensitive mechanisms due respectively to Koenderink and van Doorn (1987, 1992b) and to Wilson and Richards (1989); increasing levels of excitation are signified by increasing lightness of the receptive-field contours. C and D, examples of the corresponding curvature-tuning functions.

sensitive units (Wilson & Richards, 1989), an example of which is illustrated in Fig. 7B.

Examples of the curvature-tuning functions for the last two mechanisms are shown by the smooth curves in Fig. 7C and D, respectively, where the maximum sensitivity of each mechanism to a curved-line stimulus is plotted as a function of the curvature of the stimulus, expressed in arbitrary units of sag. As the dimensions of the receptive fields vary, the positions of the peaks and the gradients of the falling sections and to a lesser extent the rising sections of the curvature-tuning functions also vary. Notwithstanding their different receptive-field structures and the fact that the mechanisms have at least seven degrees of freedom each, the classes of curvature-tuning functions they each generate are similar. Since the curvature-tuning function determines the relevant behaviour of the mechanism, it was the form of this function that was therefore optimized, rather than the dimensions of a particular receptive-field structure. This approach reduced the degrees of freedom to three: the position of the peak of the curvature-tuning function along the curvature continuum and the gradients of the rising and falling sections of the function.

4.2. Curvature-tuning functions

For the present purpose, a curvature-sensitive mechanism was assumed to be activated by a curved-line stimulus of curvature c according to a probability $p(c)$, where p depends on the mechanism's curvature-tuning function. This probability function was modelled by an asymmetric normal function. Thus, for a curvature-sensitive mechanism i with peak sensitivity at a non-zero curvature value c_i (its preferred curvature), the probability $p_i(c)$ of activity in response to a curved line of curvature c was defined by

$$p_i(c) = \begin{cases} \exp[-k_1^2(c - c_i)^2], & \text{for } c \leqslant c_i, \\ \exp[-k_2^2(c - c_i)^2], & \text{for } c > c_i, \end{cases}$$

where the slopes k_1, k_2 of the rising and falling sections of the function each side of c_i were in general different. For mechanisms with zero preferred curvature, that is, maximally sensitive to straight lines, the slopes were set to a common value k_0. It was not assumed that these mechanisms were necessarily part of the same receptive-field family as those with non-zero preferred curvature. Replacing the normal function by a Cauchy function $[1 + k^2(c - c_i)^2]^{-1}$ or by a truncated quadratic function $\max\{0, 1 - k^2(c - c_i)^2\}$ produced similar performances.

4.3. Generating hits and false alarms

Data for the two orientation configurations were analysed independently. For vertically oriented curved lines, it was assumed that there were $2m + 1$ categories

of vertically oriented curvature-sensitive mechanisms, with preferred curvatures c_i spaced at equal intervals, $\Delta c > 0$ say, along the curvature range, that is, $-m\Delta c, \ldots, 0, \ldots, m\Delta c$, and with slopes k_1, k_2 for $c_i \neq 0$ and k_0 for $c_i = 0$. The intervals Δc could be made sufficiently small and m sufficiently large that the set of sample points effectively defined a continuum. It was assumed that each of these categories of mechanisms was distributed spatially uniformly, thereby defining a map of activity over the visual field for each preferred curvature $c_i = -m\Delta c, \ldots, 0, \ldots, m\Delta c$. For randomly oriented curved lines, it was assumed that there were $m + 1$ such categories of curvature-sensitive mechanisms with preferred curvatures $0, \ldots, m\Delta c$, but with orientations distributed uniformly in the frontoparallel plane. The values of m, $\Delta c, k_0, k_1, k_2$ were not assumed to be necessarily the same as for vertically oriented mechanisms.

Given the prior information that a target array contained one and only one curved line that differed from the rest, it was sufficient to determine whether any map i contained one and only one active element. This singular activity was assumed to underlie the perceived pop-out effect. For computational purposes, if a mechanism's activity is represented as 0 or 1, then detecting whether one and only one mechanism is active amounts to calculating whether the activity in a single map sums to unity. Notice that this calculation does not require knowledge of the spatial disposition of the curved lines in the array or their total number.

4.4. Optimizing performance

There were six parameters to the model. Five have already been defined: the number m of categories of (positive) curvature-sensitive mechanisms, the spacing Δc along the curvature continuum of the preferred curvatures of the mechanisms, and the slopes k_0, k_1, and k_2 of the rising and falling sections of the symmetric and asymmetric curvature-tuning functions. To allow for some uncertainty in the absolute positions of the curvature-tuning functions along the curvature continuum, the preferred curvatures of the mechanisms

being activated were assumed to vary randomly by a small amount from trial to trial (see e.g. Andrews, 1967). The standard deviation, σ say, of this variation, which was assumed to be normal, constituted the sixth parameter.

For each combination of target and distractor curvatures and number of distractors, an estimate $\widehat{d'}$ of target detectability was computed, based on the same number of target and non-target trials as in the experiment. The parameters of the model $m, \Delta c, k_0, k_1, k_2$, and σ were optimized with an adaptation of Brent's method to produce the best fit of $\widehat{d'}$ to the observed values of d' over all combinations of target and distractor curvatures and numbers of distractors: 315 combinations for vertically oriented curved lines and 175 combinations for randomly oriented curved lines.

The continuous lines in Figs. 3 and 5 show the optimized values of estimated target detectability $\widehat{d'}$ for vertically and randomly oriented curved lines, respectively. Although based on just six parameters, the model curves capture the data trends identified in Section 3.3, namely (1) the approximate uniformity of the dependence of target detectability on target curvature over distractor number for small distractor curvatures; (2) the asymmetry in target detectability with respect to interchange of target and distractor curvatures for large distractor numbers; and (3) the approximate uniformity of the dependence of target detectability on the difference between target and distractor curvatures over distractor curvature for small distractor numbers. The model curves also capture, to a limited extent, the secondary asymmetry when there are just two curved lines in the target array (Figs. 3 and 5, bottom row), with higher $\widehat{d'}$ values for target and distractor curvatures of respectively 10 and 0 arcmin (Fig. 3, value fitted to data point A) than with target and distractor curvatures of respectively 0 and 10 arcmin (Fig. 3, value fitted to data point E). As with the experimental data, the asymmetry is attributable to the differences in the FARs for the corresponding non-target arrays. The quantitative fits of the model are, however, imperfect. There is a significant residual variance for both vertically and randomly ori-
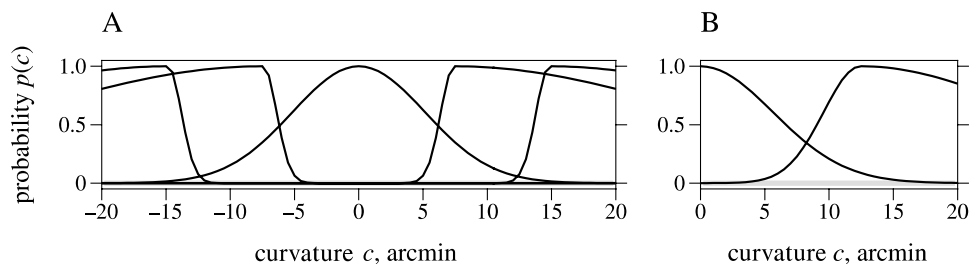

Fig. 8. Optimal curvature-tuning functions of a categorical model of curved-line detection for (A) vertically oriented curved lines and (B) randomly oriented curved lines. Each function describes the probability of the underlying mechanism generating activity in response to a curved-line stimulus of curvature c. The equation of each function is given in Section 4.2, and parameter values in Table 1.

Table 1
Parameter values for a categorical model of curved-line detection

Parameter	Curved-line orientation	
	Vertical	Random
Spacing Δc	7.4 arcmin	12.5 arcmin
Symmetric common slope k_0	0.14 arcmin^{-1}	0.13 arcmin^{-1}
Asymmetric rising slope k_1	0.69 arcmin^{-1}	0.24 arcmin^{-1}
Asymmetric falling slope k_2	0.037 arcmin^{-1}	0.043 arcmin^{-1}
SD σ of location	2.7 arcmin	3.3 arcmin

The model curvature-tuning functions were based on asymmetric normal functions spaced at intervals Δc along the curvature continuum and on one symmetric normal function centred at zero curvature. Curvature and reciprocal curvature were quantified in terms of sag (arcmin visual angle). Parameter values were optimized separately for vertically and randomly oriented curved lines. For details, see Section 4.

ented curved lines ($F(310, 1550) = 3.1$; $F(170, 850) = 1.8$, respectively), although the RMSEs are not excessive (0.41 and 0.33 respectively).

Fig. 8 shows the corresponding curvature-tuning functions for (A) vertically oriented curved lines, for which three categories suffice (five if signed curvatures are included) and (B) randomly oriented curved lines, for which two categories suffice. The values of the five parameters $\Delta c, k_0, k_1, k_2$, and σ are listed in Table 1 for vertically and randomly oriented curved lines. As with the examples in Fig. 7, the rising sections of the tuning functions for mechanisms with non-zero preferred curvature are much steeper than the falling sections ($k_1 \gg k_2$) and steeper also than the rising and falling sections of the tuning function for mechanisms with zero preferred curvature ($k_1 > k_0$).

For mechanisms with zero preferred curvature, the curvature-tuning functions are almost identical with vertically oriented and randomly oriented curved lines, but, for mechanisms with non-zero preferred curvature, they differ: the tuning functions are sharper and more closely spaced with vertically oriented than with randomly oriented curved lines (compare values of k_1 and of σ in Table 1).

5. General discussion

Rapid curved-line-target detection in multi-element arrays depends on the curvature of the target, on the curvature of the distractors, and on the total number of curved lines in the field. Yet, as shown here, the pattern of uniformities and asymmetries in the data can be largely explained by a simple model of rapid, parallel, curved-line detection in which contour curvature is coded in terms of just two or three curvature categories, depending on curved-line orientation. The curvature-tuning functions of the mechanisms assumed to underlie this performance are relatively broad, and highly asymmetric when the preferred curvatures of the mechanisms are non-zero, presumably reflecting the

geometry of their underlying receptive-field structures. It is suggested that this curvature-tuning asymmetry is the cause of the target–distractor response asymmetry. Thus, in essence, mechanisms with positive preferred curvature are strongly sensitive to curved lines but not to straight lines, whereas mechanisms with zero preferred curvature are strongly sensitive to both straight and curved lines; hence, a curved-line target in an array of many straight-line distractors produces a strong signal with little noise in the map (or maps) of curved-line activity, whereas a straight-line target in an array of curved-line distractors produces a strong signal accompanied by strong distractor noise in a map of straight-line activity. It is stressed that this model is minimal, and it may be possible to account better for the data with more than two or three categories of curvature-sensitive mechanisms with suitable receptive-field structures (cf. Foster & Westland, 1998, for oriented-line-target detection with multiple orientation-sensitive mechanisms).

Although this model was able to explain detection performance with vertically and randomly oriented curved lines, there were differences in the parameter values obtained with the two orientation configurations: the tuning functions were sharper and more closely spaced with vertically oriented than with randomly oriented curved lines, a result which suggests that curvature coding is indeed confounded with orientation coding (Simmons & Foster, 1992). This is not to imply that curvature is itself necessarily derived from elementary orientation cues; rather, that the representation of curvature of curved lines is a vector quantity, linked, for example, to the orientation and direction (sign) of the normal to the chord. [5] Such a linkage might occur if the maps of activity for each preferred curvature were different for different orientations. Comparison of curved lines with different orientations would entail comparisons collapsed across different maps, a potentially more noisy process.

In accounting quantitatively for observed detection performance, the model was least successful with multiple distractors of intermediate curvature and intermediate number and with just one distractor of very small curvature. With just one distractor, target detectability might have been determined not by the pop-out process described in Section 4.3 but by more continuous kinds of coding, based, for example, on a cross-correlation of activity associated with pairs of curved lines (target and distractor) over all curvature categories. Although such a calculation can explain target-detection functions with one distractor, it was found to fail rapidly as the number of distractors increased.

---

[5] There is also an oblique effect for curvature discrimination (Ogilvie & Daicar, 1967; Watt & Andrews, 1982; Wilson, 1985), which might also produce a confound.

It is unclear how this pattern of target-detection performance might change with curved lines that have chords longer or shorter than those used here, or for stimuli presented more centrally within the visual field, or drawn from a larger or smaller continuum. For oriented-line-target detection, there is evidence of a decline in parallel processing as line length is reduced from 1.0° visual angle to 0.25° (Doherty & Foster, 1999), but, in a previous study of curved-line-target detection in briefly presented masked arrays of just four curved lines with chord lengths of 0.2° and spaced at 2.0°, performance was clearly categorical. The largest value of preferred curvature of the underlying mechanisms was about 4 arcmin (Fig. 5a in Foster, 1983; see also Ferraro & Foster, 1986, Figs. 2 and 3), which is smaller than the value of 7–13 arcmin obtained with the larger and more widely spaced stimuli used here. Range effects seemed to have little influence on the pattern of curved-line discrimination performance (Foster, 1983).

Fast parallel mechanisms for detecting differences in contour curvature could contribute to early scene segmentation, influencing both planar and three-dimensional shape perception (Attneave, 1954; Lamote & Wagemans, 1999; Levin, Takarae, Miner, & Keil, 2001; Richards, Dawson, & Whittington, 1986; Richards, Koenderink, & Hoffman, 1987), although the perception of surface curvature from shading information (e.g. Johnston & Passmore, 1994; Koenderink & van Doorn, 1992a) is likely to be mediated by mechanisms with receptive-field structures very different from those sketched in Fig. 7. Nevertheless, there is some evidence for a discrete visual coding of surface curvature or of a related attribute. Preliminary data from target-detection experiments with arrays of two-dimensional rendered hemispherical objects suggest that performance over a range of surface curvatures can be accounted for by just two categories of mechanisms sensitive to surface curvature (Doherty & Foster, 1998).

Acknowledgements

References

Andrews, D. P. (1967). Perception of contour orientation in the central fovea, Part 1: short lines. *Vision Research, 7*, 975–997.

Andrews, D. P., Butcher, A. K., & Buckley, B. R. (1973). Acuities for spatial arrangement in line figures: human and ideal observers compared. *Vision Research, 13*, 599–620.

Attneave, F. (1954). Some informational aspects of visual perception. *Psychological Review, 61*, 183–193.

Beck, J. (1973). Similarity grouping of curves. *Perceptual and Motor Skills, 36*, 1331–1341.

Bergen, J. R., & Julesz, B. (1983). Parallel versus serial processing in rapid pattern discrimination. *Nature, 303*, 696–698.

Blakemore, C., & Over, R. (1974). Curvature detectors in human vision? *Perception, 3*, 3–7.

Bühler, K. (1913). *Die Gestaltwahrnehmungen: experimentelle Untersuchungen zur psychologischen und ästhetischen Analyse der Raum- und Zeitanschauung.* Stuttgart: W. Spemann.

Carrasco, M., Mclean, T. L., Katz, S. M., & Frieder, K. S. (1998). Feature asymmetries in visual search: effects of display duration, target eccentricity, orientation and spatial frequency. *Vision Research, 38*, 347–374.

Della Valle, L., Andrews, T. G., & Ross, S. (1956). Perceptual thresholds of curvilinearity and angularity as functions of line length. *Journal of Experimental Psychology, 51*, 343–347.

Dobbins, A., Zucker, S. W., & Cynader, M. S. (1987). Endstopped neurons in the visual cortex as a substrate for calculating curvature. *Nature, 329*, 438–441.

Dobbins, A., Zucker, S. W., & Cynader, M. S. (1989). Endstopping and curvature. *Vision Research, 29*, 1371–1387.

Doherty, L. M., & Foster, D. H. (1998). Rapid detection of shaded curved-surface targets: performance asymmetry and categorical processing. *Perception, 27*(Suppl), 37.

Doherty, L. M., & Foster, D. H. (1999). Limitations of rapid parallel processing in the detection of long and short oriented line targets. *Spatial Vision, 12*, 485–497.

Doherty, L. M., & Foster, D. H. (2001). Reference frame for rapid visual processing of line orientation. *Spatial Vision, 14*, 121–137.

Ferraro, M., & Foster, D. H. (1986). Discrete and continuous modes of curved-line discrimination controlled by effective stimulus duration. *Spatial Vision, 1*, 219–230.

Foster, D. H. (1980). A spatial perturbation technique for the investigation of discrete internal representations of visual patterns. *Biological Cybernetics, 38*, 159–169.

Foster, D. H. (1983). Visual discrimination, categorical identification, and categorical rating in brief displays of curved lines: implications for discrete encoding processes. *Journal of Experimental Psychology—Human Perception and Performance, 9*, 785–806.

Foster, D. H., & Ward, P. A. (1991). Asymmetries in oriented-line detection indicate two orthogonal filters in early vision. *Proceedings of the Royal Society of London, Series B, 243*, 75–81.

Foster, D. H., Simmons, D. R., & Cook, M. J. (1993). The cue for contour-curvature discrimination. *Vision Research, 33*, 329–341.

Foster, D. H., & Simmons, D. R. (1994). Viewpoint-invariance of contour-curvature discrimination over extended performance levels. *Spatial Vision, 8*, 45–55.

Foster, D. H., & Westland, S. (1998). Multiple groups of orientation-selective visual mechanisms underlying rapid orientated-line detection. *Proceedings of the Royal Society of London, Series B, 265*, 1605–1613.

Foster, D. H., Savage, C. J., Mannan, S., & Ruddock, K. H. (2000). Asymmetries of saccadic eye movements in oriented-line-target search. *Vision Research, 40*, 65–70.

Green, D. M., & Swets, J. A. (1966). *Signal detection theory and psychophysics.* New York: Wiley.

Gurnsey, R., Humphrey, G. K., & Kapitan, P. (1992). Parallel discrimination of subjective contours defined by offset gratings. *Perception & Psychophysics, 52*, 263–276.

Johnston, A., & Passmore, P. J. (1994). Shape from shading, I: surface curvature and orientation. *Perception, 23*, 169–189.

Koenderink, J. J., & van Doorn, A. J. (1987). Representation of local geometry in the visual system. *Biological Cybernetics, 55*, 367–375.

Koenderink, J. J., & van Doorn, A. J. (1992a). Surface shape and curvature scales. *Image and Vision Computing, 10*, 557–565.

Koenderink, J. J., & van Doorn, A. J. (1992b). Generic neighborhood operators. *IEEE Transactions on Pattern Analysis and Machine Intelligence, 14*, 597–605.

Kramer, D., & Fahle, M. (1996). A simple mechanism for detecting low curvatures. *Vision Research, 36*, 1411–1419.

Kramer, D., & Fahle, M. (1998). A simple mechanism for detecting low curvatures (Vol. 36, pp. 1411, 1996). *Vision Research, 38*, 773.

Lamote, C., & Wagemans, J. (1999). Rapid integration of contour fragments: from simple filling-in to parts-based shape description. *Visual Cognition, 6*, 345–361.

Levin, D. T., Takarae, Y., Miner, A. G., & Keil, F. (2001). Efficient visual search by category: specifying the features that mark the difference between artifacts and animals in preattentive vision. *Perception & Psychophysics, 63*, 676–697.

Li, Z. P. (1999). Contextual influences in V1 as a basis for pop out and asymmetry in visual search. *Proceedings of the National Academy of Sciences of the United States of America, 96*, 10530–10535.

Ogilvie, J., & Daicar, E. (1967). The perception of curvature. *Canadian Journal of Psychology, 21*, 521–525.

Richards, W., Dawson, B., & Whittington, D. (1986). Encoding contour shape by curvature extrema. *Journal of the Optical Society of America A, 3*, 1483–1491.

Richards, W. A., Koenderink, J. J., & Hoffman, D. D. (1987). Inferring three-dimensional shapes from two-dimensional silhouettes. *Journal of the Optical Society of America A, 4*, 1168–1175.

Rouder, J. N. (2000). Assessing the roles of change discrimination and luminance integration: evidence for a hybrid race model of perceptual decision making in luminance discrimination. *Journal of Experimental Psychology—Human Perception and Performance, 26*, 359–378.

Sagi, D., & Julesz, B. (1987). Short-range limitation on detection of feature differences. *Spatial Vision, 2*, 39–49.

Shepard, R. N., & Cermak, G. W. (1973). Perceptual-cognitive explorations of a toroidal set of free-form stimuli. *Cognitive Psychology, 4*, 351–377.

Simmons, D. R., & Foster, D. H. (1992). Segmenting textures of curved-line elements. In G. A. Orban, & H.-H. Nagel (Eds.), *Artificial and biological vision systems* (pp. 324–349). Berlin: Springer-Verlag.

Treisman, A. (1985). Preattentive processing in vision. *Computer Vision, Graphics, and Image Processing, 31*, 156–177.

Treisman, A., & Gormican, S. (1988). Feature analysis in early vision: evidence from search asymmetries. *Psychological Review, 95*, 15–48.

Treisman, A. M., Sykes, M., & Gelade, G. (1977). Selective attention and stimulus integration. In S. Dornic (Ed.), *Attention and Performance VI* (pp. 333–361). Hillsdale, New Jersey: Lawrence Erlbaum Associates.

Watt, R. J., & Andrews, D. P. (1982). Contour-curvature analysis: hyperacuities in the discrimination of detailed shape. *Vision Research, 22*, 449–460.

Watt, R. J. (1984). Further evidence concerning the analysis of curvature in human foveal vision. *Vision Research, 24*, 251–253.

Watt, R. J., Ward, R. M., & Casco, C. (1987). The detection of deviation from straightness in lines. *Vision Research, 27*, 1659–1678.

Whitaker, D., Latham, K., Makela, P., & Rovamo, J. (1993). Detection and discrimination of curvature in foveal and peripheral vision. *Vision Research, 33*, 2215–2224.

Whitaker, D., & McGraw, P. V. (1998). Geometric representation of the mechanisms underlying human curvature detection. *Vision Research, 38*, 3843–3848.

Wiesel, T. N., & Gilbert, C. D. (1989). The Helmerich Lecture: neural mechanisms of visual perception. In D. M.-K. Lam, & C. D. Gilbert (Eds.), *Second retina research foundation symposium* (Vol. 2) (pp. 7–33). The Woodlands, TX: Portfolio Publishing Company, The Woodlands, TX: Gulf Publishing Company, Houston, TX.

Wilson, H. R. (1985). Discrimination of contour curvature: data and theory. *Journal of the Optical Society of America A, 2*, 1191–1198.

Wilson, H. R., & Richards, W. A. (1989). Mechanisms of contour curvature discrimination. *Journal of the Optical Society of America A, 6*, 106–115.

Wolfe, J. M., Friedman-Hill, S. R., Stewart, M. I., & O'Connell, K. M. (1992a). The role of categorization in visual search for orientation. *Journal of Experimental Psychology—Human Perception and Performance, 18*, 34–49.

Wolfe, J. M., Yee, A., & Friedman-Hill, S. R. (1992b). Curvature is a basic feature for visual search tasks. *Perception, 21*, 465–480.

Zanker, J. M., & Quenzer, T. (1999). How to tell circles from ellipses: perceiving the regularity of simple shapes. *Naturwissenschaften, 86*, 492–495.